Developmental Cell
Article

Apoptotic Cells Provide an Unexpected Source of Wnt3 Signaling to Drive *Hydra* Head Regeneration

Simona Chera,[1] Luiza Ghila,[1,2] Kevin Dobretz,[1] Yvan Wenger,[1] Christoph Bauer,[2] Wanda Buzgariu,[1] Jean-Claude Martinou,[3] and Brigitte Galliot[1,*]
[1]Department of Zoology and Animal Biology
[2]National Center of Competence in Research "Frontiers in Genetics"
[3]Department of Cell Biology
University of Geneva, 30 Quai Ernest Ansermet, CH-1211 Geneva 4, Switzerland
*Correspondence: brigitte.galliot@unige.ch
DOI 10.1016/j.devcel.2009.07.014

SUMMARY

Decapitated *Hydra* regenerate their heads via morphallaxis, i.e., without significant contributions made by cell proliferation or interstitial stem cells. Indeed, *Hydra* depleted of interstitial stem cells regenerate robustly, and Wnt3 from epithelial cells triggers head regeneration. However, we find a different mechanism controlling regeneration after midgastric bisection in animals equipped with both epithelial and interstitial cell lineages. In this context, we see rapid induction of apoptosis and Wnt3 secretion among interstitial cells at the head- (but not foot-) regenerating site. Apoptosis is both necessary and sufficient to induce Wnt3 production and head regeneration, even at ectopic sites. Further, we identify a zone of proliferation beneath the apoptotic zone, reminiscent of proliferative blastemas in regenerating limbs and of compensatory proliferation induced by dying cells in *Drosophila* imaginal discs. We propose that different types of injuries induce distinct cellular modes of *Hydra* head regeneration, which nonetheless converge on a central effector, Wnt3.

INTRODUCTION

The freshwater polyp *Hydra* is a classical model system to investigate the cellular and molecular basis of regeneration. *Hydra* exhibits a tube shape, with a mouth opening surrounded by tentacles at the oral end (head) and a basal disc or foot at the aboral pole. Its cellular organization is simple; myoepithelial cells constitute the endoderm and ectoderm layers, whereas the intermingled interstitial stem cells differentiate into neurons, mechano-sensory cells (nematocytes), gland cells, and gametes (Steele, 2002). Therefore, three distinct stem cell populations, endodermal epithelial (digestive), ectodermal epithelial, and interstitial, permanently self-renew and differentiate in the adult polyp, and interstitial cells (i-cells) form a heterogeneous population including stem cells and early precursors for the neuronal, nematocyte, and gland cell lineages (see Figure S1A available online). Classically, head regeneration in *Hydra* is defined as morphallactic, i.e., occurring in the absence of cell proliferation (Park et al., 1970; Holstein et al., 1991), and de novo morphogenesis mostly relies on the myoepithelial cells (Fujisawa, 2003). Transplantation experiments showed that a head-organizer activity arises in head-regenerating (HR) tips after 2 hr, reaching a plateau value by 10 hr postamputation (hpa) (MacWilliams, 1983). The "early" genes, which are transiently upregulated in regenerating tips during that period, are candidates to deploy this head-organizer activity (Galliot et al., 2006). Among those, the CREB transcription factor is immediately phosphorylated by RSK in head- but not foot-regenerating tips (Kaloulis et al., 2004), whereas *Wnt3*, *β-catenin*, and *Tcf* show a locally induced upregulation (Hobmayer et al., 2000). Pharmacological evidence indicated that both pathways are likely required for setting up the head-organizer activity in *Hydra* (Galliot et al., 1995; Kaloulis et al., 2004; Broun et al., 2005; Guder et al., 2006b), the MAPK/CREB pathway supporting a key function in the initiation phase of head regeneration. Here we show that bisection at midgastric level induces apoptosis specifically in head-regenerates. These apoptotic cells release Wnt3 that is required and sufficient for head regeneration. Ectopic induction of apoptosis in the regenerating foot is sufficient to cause head formation. These results highlight an unexpected way to activate Wnt signaling for head regeneration in *Hydra*.

RESULTS

Immediate Apoptosis in Head-Regenerating Tips

To study apoptosis during regeneration, we bisected *Hydra* at mid-gastric level and examined TUNEL staining at 1 hpa in both the regenerating head and foot halves. In the upper halves, the numerous TUNEL+ cells detected along the tentacles were also present in intact *Hydra* (data not shown), indicating a process that is regeneration-independent. To our surprise, a zone of apoptotic cells was detected at 1 hpa in the head-regenerate that was absent in the foot-regenerate (Figure 1A). To further characterize this apoptotic event, regenerating halves taken from 1 up to 16 hpa were sliced to macerate separately the regenerating tips (about 100 μm deep; see Figure 1A). Cellular staining of macerated tissue is a common procedure in *Hydra* that preserves cell morphology (David, 1973). In

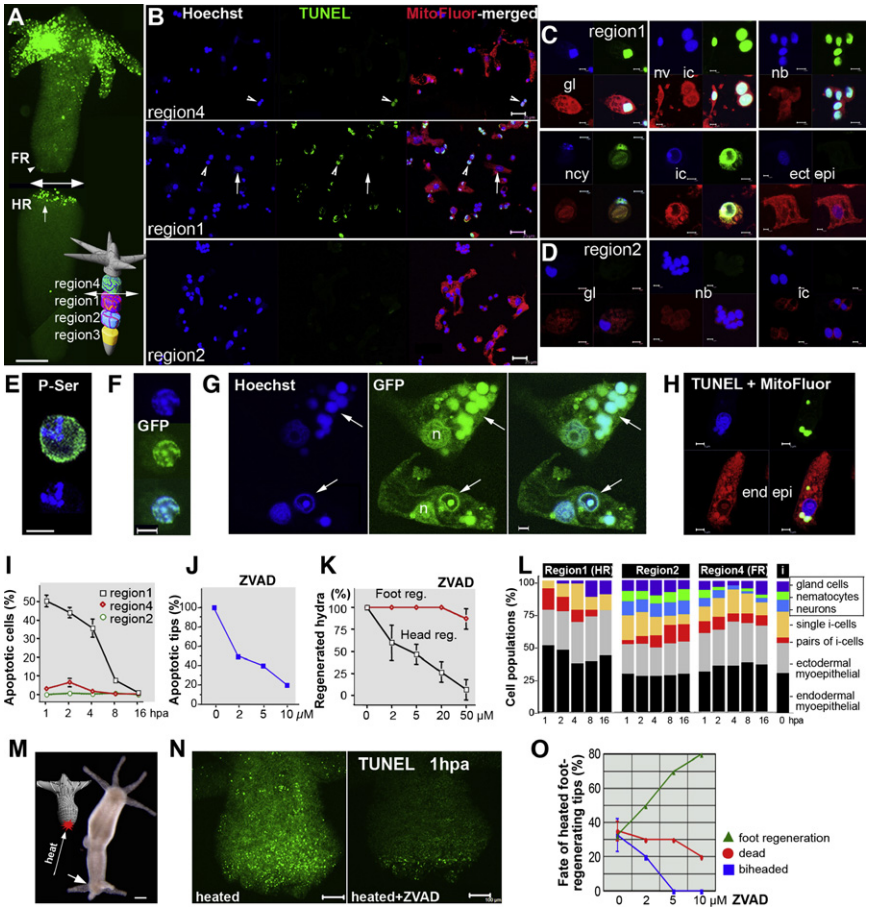

Figure 1. Amputation Triggers Apoptosis in Head- but Not Foot-Regenerating Tips

(A) TUNEL detection of numerous apoptotic cells in head-regenerating tips (HR, arrow) at 1 hpa. Note the absence of TUNEL+ cells in foot-regenerating tips (FR, arrowhead). The scheme depicts the slicing procedure performed on regenerates at various time points to macerate separately the different regions as applied in (B)–(H).

(B–D) TUNEL detection of apoptotic cells (green) in macerated region1, region2, and region4 at 1 hpa. Cells were costained with Hoechst (blue) and MitoFluor (red). Note the high density of apoptotic cells in region1 (arrowheads) and the absence of apoptotic epithelial cells (arrows). (C and D) Enlarged views of region1 (C) and region2 (D) showing ectodermal epithelial cell (ect epi), gland cell (gl), interstitial cell (ic), clustered nematoblasts (nb), nematocyte (ncy), and neuron (nv).

(E) Annexin-V detection of apoptotic cells in region1.

(F and G) Detection at 45 min pa of GFP+ apoptotic cells (F) and engulfed GFP+ apoptotic bodies ([G], arrows) in region1 from the AEP Icy1 strain that constitutively expresses eGFP in i-cells (Khalturin et al., 2007); n: nucleus.

(H) TUNEL+ apoptotic bodies engulfed in a digestive cell (end epi).

(I) Percentage of apoptotic cells identified in head- and foot-regenerating tips after maceration and Hoechst staining (Table S2).

(J and K) ZVAD treatment (10 μM) inhibits apoptosis in region1 (J) and head regeneration (K) recorded at 2 hpa and 72 hpa, respectively.

(L) Cell-type distribution of the nonapoptotic cells in regions 1, 2, and 4 from 1 to 16 hpa and in intact *Hydra* (i). *Hydra* differentiates a dozen of cell types (Figure S1A) that were identified and quantified on macerates after Hoechst staining and CREB and RSK immunostaining (Figures S1G–S1M). Note the absence of neurons and nematocytes (boxed names) from region1 at all time points. In (I) and (L) the mean values ± SD were obtained by counting at least 1800 cells per condition in 3 independent experiments (Tables S2 and S4).

(M) Schematic representation of the heating procedure to induce ectopic apoptosis (left, red star) and biheaded *Hydra* obtained 3 days after bisection and immediate heating of region4 (arrow).

(N) Local heating dramatically increases apoptosis in region4 as detected by TUNEL at 1 hpa (left), but this induction is inhibited upon ZVAD treatment (right).

(O) Head regeneration from heated upper halves is inhibited upon ZVAD in a dose-dependent manner. Scale bars (μm): 200 (A), 25 (B), 5 (C–H), 100 (M and N).

macerated HR tips, the presence of numerous apoptotic cells was confirmed at 1 hpa by TUNEL analysis (Figures 1B–1D; see Figures S1C and S1D). Moreover chromatin condensation, nuclear fragmentation, and apoptotic bodies were detected with Hoechst (Figure S1G) and Annexin-V (Figure 1E) staining. When we used the transgenic Icy1 strain that constitutively expresses eGFP in i-cells (Khalturin et al., 2007), we found eGFP+ apoptotic nuclei in macerates (Figure 1F) as well as eGFP+ apoptotic bodies engulfed by digestive cells (Figure 1G). Digestive cells with engulfed apoptotic bodies could also be traced after TUNEL (Figure 1H) and in TEM views of regenerating tips at 2 hpa (Figure S1B).

To quantify this apoptotic event, the proportion of apoptotic nuclei was compared in distinct regions of the regenerating halves after maceration: in HR tips 50% of the cells displayed typical hallmarks of apoptosis at 1 hpa (Figure 1I), whereas the number of late-apoptotic cells, i.e., already forming apoptotic bodies, increased from 15% to 52% over the first 4 hr (Table S3). This percentage decreased in the next 3 hr to further drop below 1% at 16 hpa, the value measured in the body column of intact polyps, indicating that apoptosis is an immediate and transient event. By contrast, in foot-regenerating (FR) tips the kinetics were similar though delayed by 2 hr, but the percentage of apoptotic cells never exceeded 7%. Moreover, in HR tips the digestive cells showed dramatic morphological modifications, progressively losing their epithelial polarity, taking an ovoid shape, and contacting the apoptotic bodies to finally engulf them (Figures S2A and S2B). At 2 hpa 88% digestive cells were metaplasic, and at 4 hpa 57% contained phagosomes (Figure S2C). A similar process, although delayed and limited to 25% of the digestive cells, was observed in FR tips (Figure S2C). Consistent with previous work (Bottger and Alexandrova, 2007), only digestive cells were observed to perform this engulfment function.

To test whether this early wave of apoptosis is required for head regeneration, we treated *Hydra* with the pan-caspase inhibitor ZVAD (Cikala et al., 1999). TUNEL+ cells were no longer detected in 80% of head-regenerates, indicating that the amputation-induced apoptosis in HR tips is caspase dependent (Figure 1J). Importantly, inhibition of apoptosis significantly

inhibited head, but not foot, regeneration (Figure 1K). Animals failing to regenerate heads in the presence of ZVAD ultimately die after a few days (see Figure 4B and associated text below for a discussion of conditions that rescue both head regeneration and overall animal survival during ZVAD treatment); however, animals treated with the same dose of ZVAD that nonetheless initiate head regeneration are then fully capable of regeneration and long-term survival. The ZVAD response is thus "all or nothing," suggesting that only a high level of immediate apoptosis specifically promotes head regeneration. To test this hypothesis, we induced apoptosis ectopically by locally heating the FR tips immediately after amputation. This resulted in the formation of double-headed *Hydra* by converting foot regeneration into head regeneration in at least 30% of the upper halves (Figure 1M, arrow). At 1 hpa we detected numerous apoptotic nuclei in the heated region, a pattern similar to that normally seen in HR tips (Figure 1N). When ZVAD was added to the heated upper halves, TUNEL+ cells were rare again (Figure 1N, right) and foot regeneration resumed in a dose-dependent manner (Figure 1O). This assay shows that lowering the levels of apoptosis blocks the onset of head regeneration (see also Figure 3E) and highlights a role for apoptosis in triggering the head regeneration program in *Hydra*.

Amputation-Induced Apoptosis Is Restricted to Interstitial Cell Derivatives

We then analyzed the cell types that undergo apoptosis and noted that apoptosis was cell-type restricted, strongly affecting i-cell derivatives, i.e., neurons, nematoblasts, nematocytes, gland cells, and some i-cells, but leaving intact a large subset of interstitial cells and the epithelial cells (Figure 1C). As a result, the interstitial derivatives were dramatically depleted at 1 hpa in HR tips, and neurons were actually still absent at 16 hpa (Figure 1L; Figure S3). The adjacent region (region2) was clearly different from HR tips, as the neuronal and nematoblast populations were not affected; moreover, we noted significant modulations of the i-cells between 1 and 16 hpa. Pairs of i-cells increased from 3.5% to 13% while the single ones decreased from 19% to 7%, suggesting that the latter were dividing to give pairs (Figure 1L). Interestingly the reverse was observed at the tip, where the single i-cells increased from 5% to 19% between 1 and 4 hpa while the pairs decreased from 16% to 9%. Hence, two adjacent regions of head-regenerates exhibit strikingly different dynamics (Figure S4). In foot-regenerates the apoptotic cells also corresponded to nematocytes and neurons but their depletion was limited, the neurons remaining visible as a dense net at all time points (Figure S3). Moreover, the ratio between single and pairs of i-cells remained rather stable (Figure 1L).

Transient Wnt3 Production in Apoptotic Cells and β-Catenin Activation in S Phase Interstitial Cells

To study how apoptosis signals head regeneration, we looked to the Wnt pathway, as it was shown to induce head formation (Guder et al., 2006a). We examined whether apoptosis induces Wnt expression in 1 hpa regenerates and immunostained regenerating halves with Wnt3 and β-catenin antibodies that cross-react with the *Hydra* Wnt3 and β-catenin proteins, respectively (Figures 5B–5D). The β-catenin antibody actually provides the expected pattern in intact *Hydra*, i.e., predominantly nuclear in the apical region and cytoplasmic and membranal along the body column (Figure S5A), as reported by Broun et al. (2005). Within the first 2 hpa, we detected two successive events in head-regenerates: first, the transient presence of Wnt3-positive cells close to the wound at 30 and 45 min pa, no longer detected at 2 hpa; then, the nuclear translocation of β-catenin that was cytoplasmic and membranal at 30 min pa, but nuclear at 2 hpa (Figures 2A–2D). Importantly, upon ZVAD exposure, Wnt3 overexpression and β-catenin nuclear translocation were suppressed (Figures 2B and 4A), suggesting that this transient wave of Wnt3 overexpression depends on the apoptotic cells.

Wnt3 immunostaining on macerates confirmed that the Wnt3-overproducing cells were restricted to the tip and corresponded exclusively to cells undergoing apoptosis (Figures 2E–2G). This result was surprising, as previous analyses had reported a later *Wnt3* gene upregulation, taking place in epithelial cells several hours after mid-gastric section (Guder et al., 2006a; Hobmayer et al., 2000). To clarify this issue, we performed semiquantitative RT-PCR analysis and measured a significant increase in *Wnt3* transcript abundance between 2 and 3 hpa (Figure 2H). Also, the analysis of HR tips detected at 4 hpa a clear increase of Wnt3 protein levels in endodermal epithelial cells (Figure 2I, left); this too was prevented by ZVAD treatment (Figure 2I, right). These results are consistent with those previously reported and indicate that the Wnt3 pathway is likely activated via two sequential mechanisms during early head regeneration, an immediate, transient mechanism in i-cells, followed by another in the endodermal epithelial cells.

To further characterize the cells where β-catenin is activated, *Hydra* were pulse-labeled with BrdU for 15 min after bisection and detected for β-catenin and BrdU at successive time points (Figures 2J–2M). At 60 min β-catenin was translocated in few BrdU+ nuclei (Figure 2M, arrows), whereas at 90 min all BrdU+ nuclei were also β-catenin+ (Figures 2L and 2M). Interestingly this synchronous nuclear translocation was taking place almost exclusively in BrdU+ cells with small or middle size nuclei (<12 μm in diameter), indicating that β-catenin was activated in cycling i-cells.

Ectopic Apoptosis Induces Head Regeneration through Wnt3/β-Catenin Signaling

To investigate whether ectopic apoptosis leads to ectopic head regeneration by activating the Wnt3/β-catenin pathway, we developed an experimental assay we named "the splitting assay" (Figures 3A and 3B). Briefly, upper halves were heated as above and subsequently cut longitudinally, one half being left alive to follow the regenerative process, the other half being fixed for cellular analysis at early time points: 50% of the split-animals were fixed at 30 min to detect the Wnt3 levels (Figures 3C–3F), whereas the other 50% were BrdU incubated after heating and fixed at 2 hpa to detect β-catenin in BrdU+ cells (Figures 3G–3J). The longitudinal section did not affect the regeneration process, as *Hydra* rapidly self-closed as a thinner tube with three tentacles instead of six. The results were extremely clear: all animals that developed a secondary head (8/16) displayed significant Wnt3 overproduction at 30 min and β-catenin activation in BrdU+ cells at 2 hpa (Figures 3C and 3G). Conversely, those that despite heating regenerated a foot (4/16) exhibited weak Wnt3 levels at 30 min and no nuclear β-catenin at 2 hpa

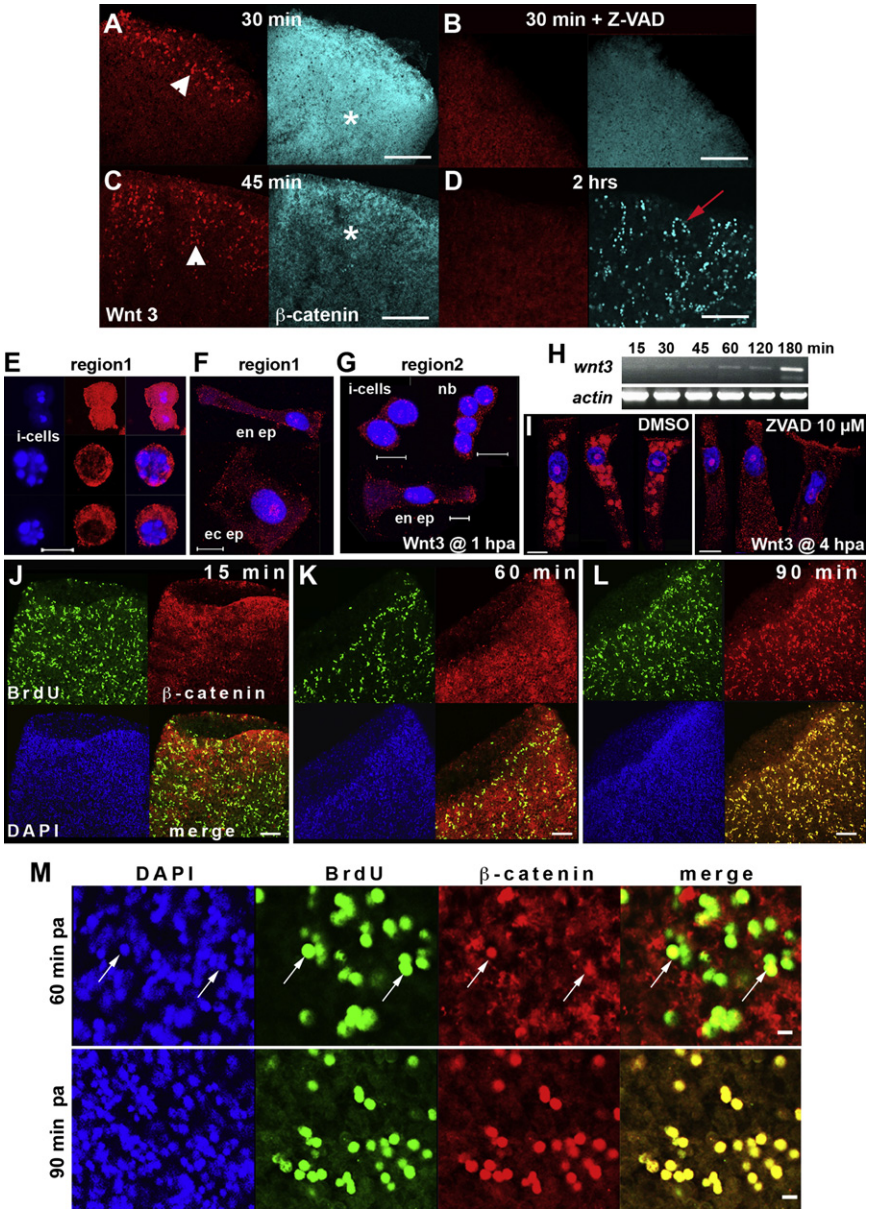

Figure 2. Wnt3 Production by Apoptotic Cells and β-Catenin Nuclear Translocation in Cycling Cells of HR Stumps

(A–D) The transient Wnt3 production ([A and C], arrowheads) observed in region1 at 30 and 45 min is inhibited in ZVAD-treated *Hydra* ([B], 10 μM). β-catenin that is cytoplasmic (blue, asterisks) at 30 and 45 min pa becomes mostly nuclear at 2 hpa ([D], red arrow).

(E–G) Wnt3 expression at 1 hpa is strong in apoptotic cells (E) but low in nonapoptotic ectodermal or endodermal epithelial cells (ec ep, en ep) from region1 (F) and in i-cells, nematoblasts (nb), and digestive cells (en ep) from region2 (G).

(H) RT-PCR detection of *Wnt3* expression in HR halves.

(I) Wnt3 protein in endodermal epithelial cells of untreated (left) or ZVAD-treated (right) HR halves at 4 hpa.

(J–M) Nuclear translocation of β-catenin (red) occurs between 60 and 90 min pa in BrdU+ cells (green, arrows). Those cells were submitted to a 15 min BrdU pulse postamputation and chased. (M) Enlarged views of (K) and (L). Scale bars (μm): 100 (A–D, and J–L), 10 (E–G, I, and M).

(Figures 3D and 3H), similarly to foot regeneration (Figures 3F and 3J). Finally, when heated upper halves were exposed to ZVAD, Wnt3 levels were very low, β-catenin was no longer nuclear translocated, and a secondary ectopic head never formed (16/16, Figures 3E and 3I). We therefore concluded that the increase in the level of apoptosis was sufficient to immediately activate the Wnt3/β-catenin pathway and convert FR tips to HR ones.

Rescue of Head Regeneration in ZVAD-Treated *Hydra* upon Wnt3 Treatment

As the previous results suggested that apoptotic cells drive head regeneration by activating the Wnt pathway, we wanted to test whether exogenously added Wnt3 could rescue head regeneration in *Hydra* inhibited for apoptosis. So we exposed ZVAD-treated *Hydra* to soluble Wnt3 from 90 min prior to bisection up to 2 hpa. We noted that Wnt3 exposure induced β-catenin nuclear translocation in a dose-dependent manner (Figure 4A; Figure S5B) and could rescue the head regeneration process in 100% of ZVAD-treated head-regenerates that otherwise would die in about 2 days (Figure 4B). The analysis of the regeneration kinetics actually showed that Wnt3 exposure drastically accelerated head regeneration, even in ZVAD-treated *Hydra*, as 60% of them had already differentiated tentacle rudiments at 28 hpa, versus less than 10% in control animals (Figure 4C). These results validate the proposed hypothesis whereby apoptosis triggers Wnt3 production, which in turn represents a quantitative effector of the head regeneration response.

Cell Proliferation Is Abolished in *Wnt(RNAi)* and *β-Catenin(RNAi) Hydra*

To test the role of the Wnt3 pathway in head regeneration, we generated *Wnt3(RNAi)* and *β-catenin(RNAi)* knocked-down *Hydra*. After 3× dsRNA feedings, the *Wnt3* and *β-catenin* transcripts were no longer detected in intact, head- or foot-regenerates exposed to the corresponding dsRNAs (Figure 5A). Some crossregulation was observed, notably in *β-catenin(RNAi) Hydra*, where *Wnt3* was upregulated during head regeneration and *Tcf* strikingly downregulated in regenerating halves. Regeneration experiments were performed 24 hr after the third feeding, as the animals did not survive longer than 3 days. Western analysis that detected Wnt3 protein produced in vitro (Figure 5B), and

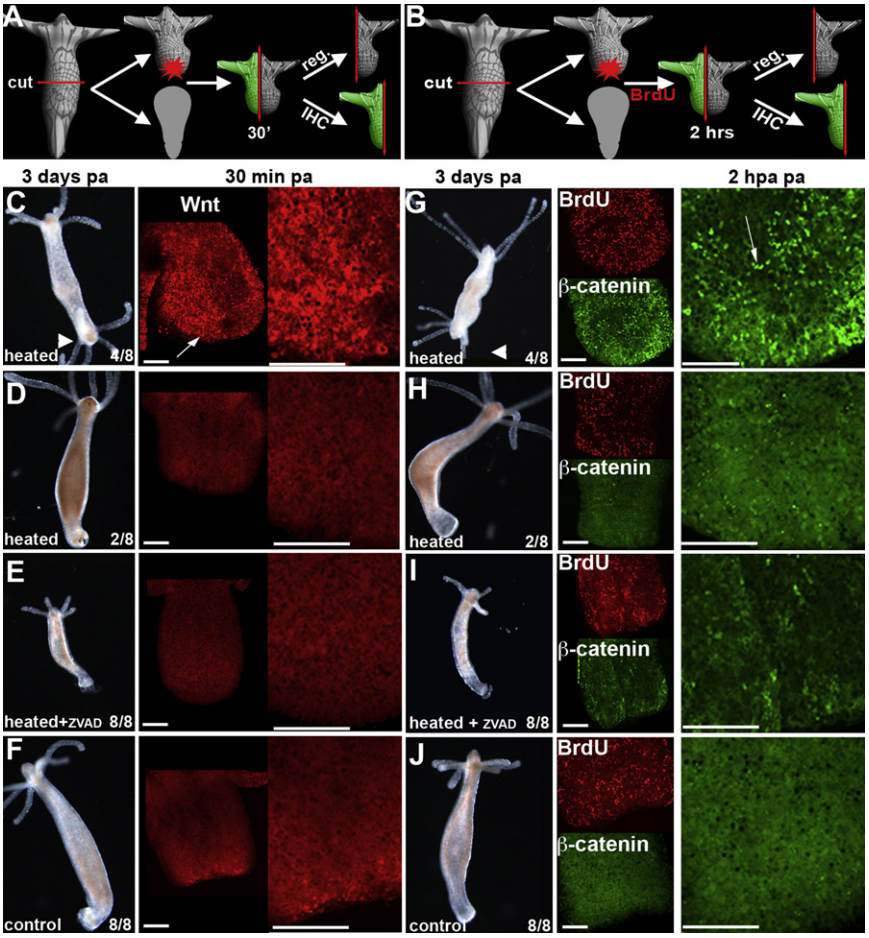

Figure 3. Ectopic Apoptosis Induces Cell Proliferation and Head Regeneration by Activating the Wnt3/β-Catenin Pathway

Scheme (A and B) depicting the splitting assay where the heated upper haves were sectioned longitudinally either at 30 min pa (A) or at 2 hpa (B). One half was left to regenerate, and the other was immediately fixed for IHC. (C–F) Wnt3-producing cells ([C], arrow) were only detected in animals that regenerate an ectopic head. (G–J) Nuclear β-catenin (green, arrow) in BrdU+ (red) cells was only detected in heated animals that regenerate an ectopic head. (C and G) Successful heat-induced ectopic heads; (D and H) unsuccessful ectopic head induction; (E and I) ZVAD-treated heated *Hydra*; (F and J) unheated control upper halves. Scale bars: 100 μm.

immunostaining failed to detect any Wnt3 from intact (Figure 5C) or regenerating (Figure 5E) *Wnt3(RNAi) Hydra*. In the absence of Wnt3 protein, β-catenin no longer translocated to the nucleus and cells stopped cycling as evidenced by the complete absence of BrdU+ cells at 2 hpa (Figure 5F).

In contrast to Wnt3, the silencing of β-catenin protein was only partial: on the day following the third dsRNA feeding, β-catenin was still detected at low levels on WCE, although not detectable on regenerates in the usual conditions of laser setting (Figures 5D–5F). However, 1 day later the intact polyps started to dissociate and die (data not shown), suggesting that they could survive as long as some β-catenin protein produced prior to RNAi persisted (a week). The *β-catenin(RNAi) Hydra* bisected the day following the third feeding were unable to regenerate but could survive the amputation stress for about 8 hr. In such animals, the Wnt3 protein was ubiquitously overexpressed along the stump but did not show the early dashed pattern usually observed at the tips (Figure 5E). Similarly to *Wnt3(RNAi)*, cell cycling was abolished after *β-catenin(RNAi)*, as evidenced by the absence of any BrdU-labeled cells (Figure 5F). These data indicate that the conventional Wnt3/β-catenin pathway is directly or indirectly required for the amputation-induced proliferative response.

Formation of a Proliferative Zone in Region2

To characterize the apoptosis-induced proliferative response, we performed a systematic analysis of cell cycling over the first 8 hpa: *Hydra* were pulse labeled with BrdU for 2 hr, either

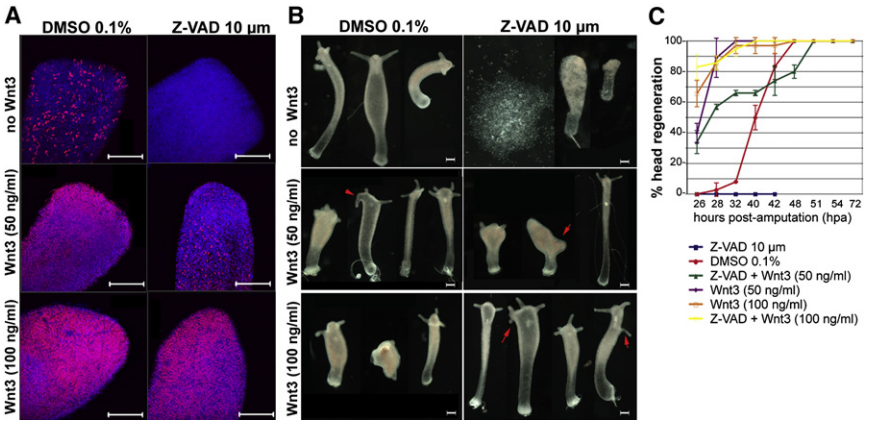

Figure 4. Wnt3 Treatment Leads to β-Catenin Activation and Rescues Head Regeneration in ZVAD-Treated *Hydra*

Hydra exposed to ZVAD or DMSO from 90 min before amputation up to 2 hpa were simultaneously treated with Wnt3 or not. (A) The level of nuclear β-catenin detected at 2 hpa correlates with the level of Wnt3 exposure (see also in Figure S5B). (B) Detection of head regeneration at 42 hpa, a time when ZVAD-treated halves are dying (the left one is dissociated). Some Wnt3-treated *Hydra* show patterning abnormalities as extra tentacles (red arrows). Scale bars: 200 μm. (C) Kinetics of head regeneration measured in three independent experiments (n = 15 in each condition). The emergence of tentacle rudiments was the criterion for assessing head regeneration. Values are represented as means ± SD (Table S6).

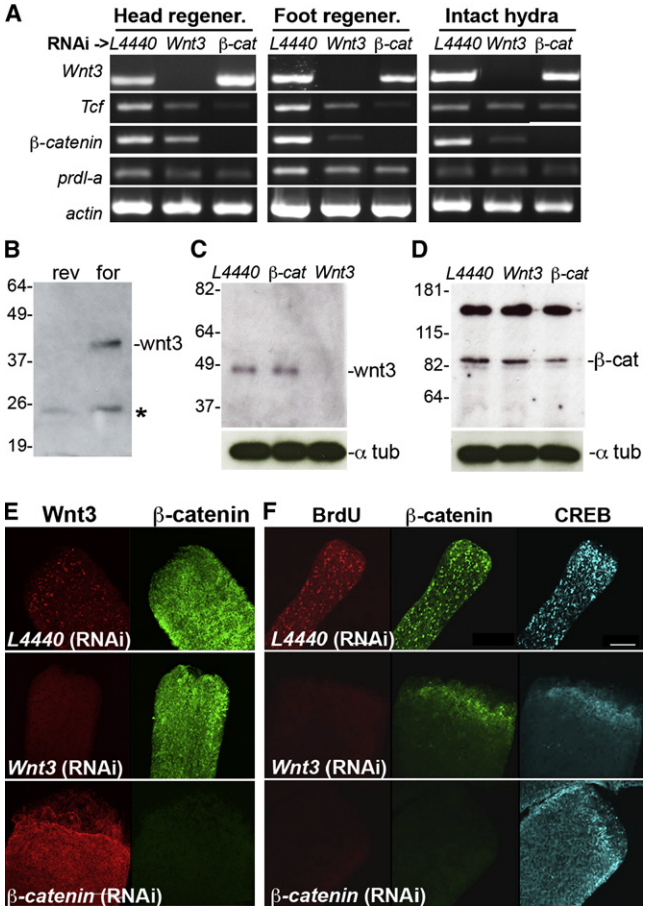

Figure 5. Lack of Amputation-Induced Proliferation in *Hydra* Knocked Down for *Wnt3* and *β-catenin*

(A) Semiquantitative RT-PCR analysis performed at 45 min pa in intact and regenerating *Hydra* exposed 3× to *L4440*, *Wnt3*, and *β-catenin* dsRNAs.

(B–D) Western blot analysis of Wnt3 (B and C) and β-catenin (D) in reticulocyte lysates that expressed the forward (for) and reverse (rev) Wnt3 cDNA constructs (B) and in WCE prepared from *L4440*, *Wnt3*, and *β-catenin* (RNAi) *Hydra* (C and D).

(E) Detection of Wnt3 (red) and β-catenin (green) in RNAi *Hydra* fixed at 30 min pa.

(F) Detection at 2 hpa of BrdU+ nuclei (red), β-catenin (green), and CREB (light blue) proteins in RNAi head-regenerates exposed for 15 min to BrdU before fixation. In (C–F), *Hydra* received dsRNAs three times. Scale bar: 150 μm.

immediately before or after bisection, up to 8 hpa. To our surprise BrdU incubation performed early after bisection revealed a high number of cycling cells in region2, detected as a proliferative zone next to the apoptotic zone with a sharp boundary (Figure 6A). To see whether ectopic apoptosis also leads to cell proliferation, we incubated locally heated upper halves in BrdU for 2 hr immediately after bisection, and indeed observed a proliferative zone adjacent to the apoptotic area (Figure 6B, brackets). This proliferative zone was no longer detected after ZVAD treatment (lower panel), the treated stumps then showing the typical homogenous distribution of BrdU+ cells observed in FR halves (Figure S6).

To quantify this proliferative response, we used the ubiquitously expressed CREB transcription factor (Chera et al., 2007) to define the BrdU-labeling index (BLI) as the proportion of BrdU+ nuclei among CREB+ nuclei counted on confocal snapshots (Table S7). The BLI was monitored every 2 hr in region1, region2, and region3 of HR halves and compared to the BLI measured in the body column of intact *Hydra* (t0 value, t0 = 31%). In *Hydra* labeled before bisection (Figure 6C, blue bars), most BrdU+ cells were apoptotic in HR tips at 2 and 4 hpa and therefore not countable; in contrast, in the lower regions the BLIs were first similar to t0 at 2 hpa, then peaked up to 43% and 44% at 4 hpa, until they became similar to t0 in region2, significantly lower than t0 in region1 (19% at 6 and 8 hpa) and region3 (24% at 6 and 8 hpa). These results suggest that cells that were in S phase prior to amputation quickly migrate from the lower part of the regenerating half toward the wound, progressively replenishing the apoptotic zone and leaving region3 rather depleted at 6 and 8 hpa. However, time-lapse studies would be needed to substantiate this possibility.

By contrast, the behavior of the cells BrdU-labeled immediately after bisection was markedly different (Figure 6C, green bars): in region2 the BLI was clearly increased at all time points, reaching 47% at 2 hpa and remaining above 50% at subsequent time points. The ratios of the BLI values obtained in *Hydra* labeled after and before bisection were 1.68, 1.26, 1.61, and 1.56 at 2, 4, 6, and 8 hpa, respectively, indicating that the number of labeled cells in region2 was significantly higher when labeling was performed after amputation. If we assume that the migration of i-cells toward the wound is similar whatever the BrdU-labeling period, then this increase in the number of labeled cells after bisection likely reflects amputation-driven processes that affect cell proliferation like S phase re-entry and/or mitosis. In the apoptotic zone (region1) the BLI of *Hydra* labeled from 0 to 2 hpa was initially very low (8% at 2 hpa), then reached a plateau value of 20% at 4 hpa, whereas in region3 the BLI first dropped down to 18% between 2 and 4 hpa, then transiently increased at 6 hpa (42%) to drop again to 26% at 8 hpa. Surprisingly, when BrdU-labeling was performed between 2 and 4 hpa, less than 11% of the cells were labeled at 4 hpa whatever the region (Figure 6C, orange bars). At subsequent time points, the BLI values ranged from 23% to 36%, closer to that observed in intact body column (Table S7). These results indicate that the dramatic increase in the number of cycling cells in region2 was strictly restricted to the first 2 hpa and that the effects on cell proliferation observed here likely reflect transient cell cycle synchronization rather than a generalized, long-term acceleration of cycling. As a consequence, the cell density at 8 hpa exhibited a 3-fold increase in region2 when compared to intact body column (Figure 6F).

To test the effect of apoptosis on cell proliferation, we exposed HR halves to ZVAD and analyzed the behavior of the BrdU+ cells (Figures 6D–6G). At 4 hpa, the ZVAD-treated halves often appeared collapsed (data not shown) and had a low BLI (<30%, whatever the labeling condition), except in region1, where the BLI reached 53% (Figures 6D, 6E, and 6G; Table S8). However, in contrast to the physiological condition, the cell density never exceeded 1.5× along Z-VAD-treated regenerating halves (Figure 6F). We suspect that in the absence of apoptosis, the cycling cells migrate toward the wound but do not receive the synchronization signal(s) that push them to divide (see below).

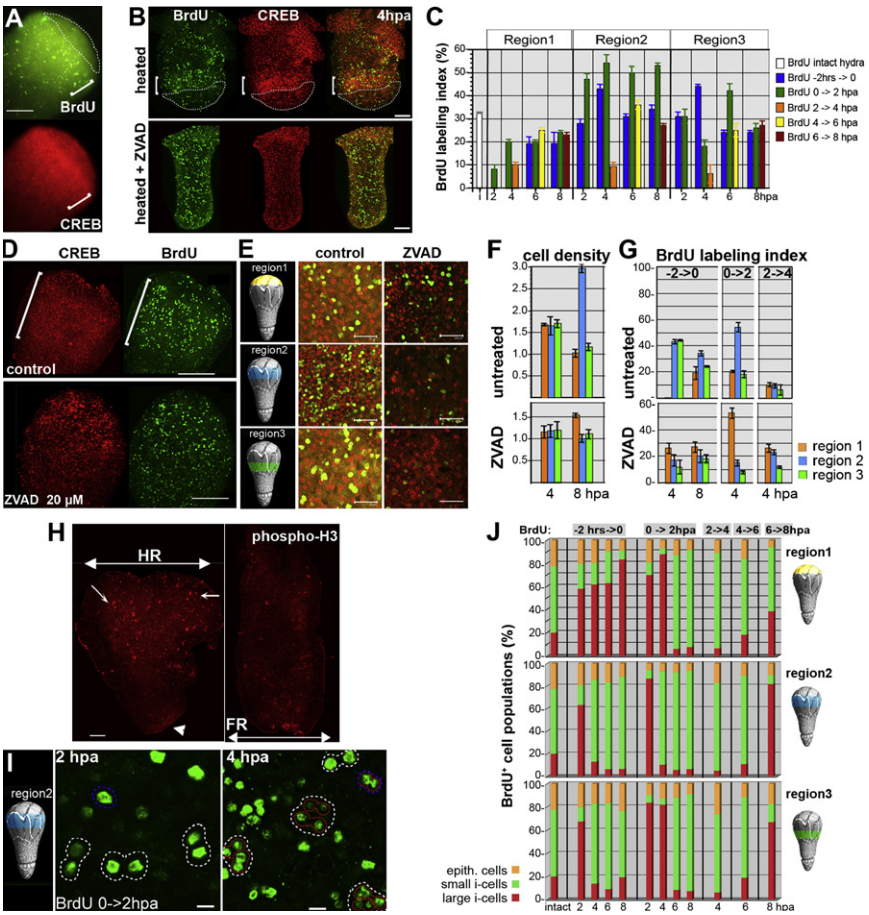

Figure 6. The Early Synchronous Division of Proliferating Cells in Head-Regenerating Stumps Is Apoptosis Dependent

(A) Detection of a proliferative zone at 4 hpa in region2 (brackets) of *Hydra* BrdU-labeled from 2 to 4 hpa and detected with the CREB (red) and BrdU (green) antibodies. A dashed line outlines region1.

(B) Detection of a proliferative zone at 4 hpa in heated upper halves exposed to BrdU from 0 to 2 hpa and immunostained as in (A). This proliferative zone does not form when ZVAD was added.

(C) Specific increase in BLI values in region2 when BrdU-labeling was performed immediately after bisection (green bars). Note the low BLI values when labeling was done between 2 and 4 hpa (orange bars, Table S7).

(D–G) The formation of the proliferative zone is altered in ZVAD-treated head-regenerates BrdU-labeled and immunostained as in (B). The BrdU+ cells (green) were less numerous and detected in region1 instead of region2 when compared to untreated *Hydra* (brackets). (E) Magnified merged views from (D). (F and G) Graphs showing cell densities (F) and BLIs (G) along head-regenerates in untreated and ZVAD-treated (20 μm) *Hydra* (Table S8). Note the 3× increase in cell density in region2 at 8 hpa in untreated *Hydra*. BrdU-labeling was performed before (−2 → 0) or after (0 → 2 hpa, 2 → 4 hpa) bisection.

(H) Mitotic cells (arrows) detected at 3 hpa with anti-phosphoH3 antibody on head- (HR) and foot-regenerating (FR) halves. Double arrow, amputation plane; arrowhead, basal disc.

(I) Pairs of BrdU+ cells (green) undergoing mitosis between 2 and 4 hpa in region2.

(J) Sorting of the BrdU+ cells between the large i-cells (red bars), small i-cells (green bars), and epithelial cells (orange bars) counted after maceration at indicated time points in regions 1, 2, and 3 (Table S9A; Figure S7). BrdU+ cells labeled before (−2 hr → 0) or after (0–2 hpa) amputation synchronously switch from large to small i-nuclei between 2 and 4 hpa in region2. Scale bars (μm): 100 (A and B), 300 (D), 50 (E), 10 (I). All values are represented as means ± SD.

Interstitial Cells Synchronously Divide between 2 and 4 hpa

Hence, several results suggested that a large fraction of the i-cells rapidly divide in region2: (1) the sustained BLI increase when labeling takes place immediately after amputation (Figure 6C), (2) the increase in the proportion of pairs of i-cells after 4 hpa (Figure 1L), and (3) the marked increase in cell density in region2 over the first 8 hpa (Figure 6F). To verify that cells indeed rapidly divide, we performed an anti-phospho-H3 staining at 3 hpa and detected a much larger number of mitotic cells in head-regenerates than in foot ones (Figure 6H).

We then analyzed on macerates the BrdU+ cell populations and noted that most BrdU+ cells from region2 were large i-cells with medium size nuclei (8–12 μm) at 2 hpa but small i-cells with small size nuclei (4–7 μm) at 4 hpa (Figure 6I; Figure S7), whereas BrdU+ epithelial cells that possess larger nuclei (>12 μm) were rare. Moreover, at 4 hpa these BrdU+ small i-cells often formed clusters of four cells, likely arising from pairs of large BrdU+ i-cells that had synchronously divided. To identify the behavior of these three BrdU+ contingents, we monitored during the 8 first hpa these three types of BrdU+ cells in region1, region2, and region3 either on macerated tissues (Figure 6J; Table S9A) or on whole mounts (Figure S7; Table S9B), and both methods provided highly similar results.

This quantification confirmed that BrdU+ cells labeled before or after bisection synchronously shift in region2 from large to small i-cells between 2 and 4 hpa with BrdU+ large i-cells >60% at 2 hpa but only 20% or less at 4 hpa (Figure 6J, red bars), while the BrdU+ small i-cells that were rare at 2 hpa increased above 70% at 4 hpa (Figure 6J, green bars). The cells labeled immediately postamputation showed a similar switch in regions 1 and 3, although delayed by 2 hr (Figure 6J), whereas the BrdU+ cells labeled prior to bisection also showed the switch behavior in region3, but not in region1, where the large i-cells were predominant at all time points (58%, 62%, 63%, and 83% on macerates), likely corresponding to surviving and migrating cells that did not undergo mitosis. By contrast the cells that had incorporated BrdU after 2 hpa exhibited distinct distributions: most of them were small i-cells at 4 and 6 hpa (Figure 6J; Figures S7E and S7F), whereas between 6 and 8 hpa mostly large i-cells incorporated BrdU in regions 2 and 3 (82% and 67% on macerates).

Hence our data suggest that i-cells traversing S phase prior to or immediately after amputation may then divide synchronously

between 2 and 4 hpa in region2 (slightly later for the cells located in regions 1 and 3 labeled from 0 to 2 hpa). These i-cells indeed appeared highly synchronized, as between 2 and 4 hpa only a very small fraction was able to traverse S phase, as deduced from the very low BLIs measured in all three regions during this period. That said, time-lapse studies would be necessary to confirm the intuitive model that the BrdU+ small i-cells observed at 4 hpa are in fact the daughters of BrdU+ large i-cells observed at 2 hpa. Overall, we propose that three events might contribute to the early formation of a proliferative zone underneath the apoptotic area: (1) the migration of i-cells (that had coincidentally initiated S phase immediately prior to amputation) from more basal regions, (2) the reentry of i-cells into the cell cycle immediately following amputation, and (3) their subsequent synchronous mitotic division by 4 hpa. Such proliferative zones were never detected in foot-regenerating halves (Figure S6).

Dynamic Modeling of the Apoptotic Cell Population

To illustrate the transient nature of the original induction of apoptosis and to obtain further insight into its early dynamics, a mathematical model composed of a system of ordinary differential equations was implemented on the different contingents of staged apoptotic cells from region1. Apoptotic cells from macerated region1 were staged at 1, 2, 4, 8, and 16 hpa as early, advanced, or late apoptotic cells, based on nuclear morphology (Table S3). Five compartments were explicitly included, corresponding to the fractions of cells in the pro-, early-, advanced-, late-, and postapoptotic stages, where postapoptotic reflects engulfed apoptotic bodies. Entry into the proapoptotic stage was described as a transient event, and subsequent transfers from one stage to another were assumed to follow first-order kinetics. The fractions of cells modeled for each stage were adjusted for the loss of cells due to the disappearance of apoptotic cells over time, and the equations describing the adjusted fractions of the experimentally counted cell populations were simultaneously optimized against measured data using the nonlinear least-squares method (see Figure S8). The resulting model predicts that the highest proportion of apoptotic cells in the early apoptotic stage (about 40%) would be detected at 30 min pa, fitting exactly with the time window when Wnt3 overproduction was detected.

DISCUSSION

The Adjacent Apoptotic and Proliferative Zones in Head-Regenerating Halves

This study identified cellular remodeling that occurs in head- but not foot-regenerating halves within the first 8 hr following mid-gastric bisection in *Hydra*. This immediate but transient remodeling involves four distinct processes according to the position from the amputation plane (Figure 7): (1) the immediate apoptosis of i-cell derivatives, which are subsequently engulfed by the surrounding digestive cells at the tip (region1), (2) the rapid accumulation of S phase cells in the vicinity of the apoptotic area (region2), (3) the migration of interstitial progenitors along the regenerating half toward the tip, and (4) the synchronous division of the cycling i-cells along the head-regenerates. Apoptosis occurs in several contexts in *Hydra* (Bottger and Alexandrova, 2007) but was never clearly established in regenerating tips. A previous report described a transient cell death induced upon wounding, but this appears a quite different process as it occurs throughout the regenerating piece and affects only differentiating nematocytes (Fujisawa and David, 1984). More similar to the remodeling described here is the metaplasia of the digestive cells that was described during the early phase of reaggregation (Murate et al., 1997), but this study does not mention a concomitant apoptotic event. The migration of i-cells was previously shown to be enhanced upon transplantation (Fujisawa et al., 1990), the progenitors migrating fast (2 μm/min) in contrast to the stem cells that show limited migration (Khalturin et al., 2007). However, it was not clear that cycling cells gather close to the wound to rapidly divide. This proliferative zone partially fulfills many criteria of a regenerative blastema, i.e., a postamputation mass of proliferative undifferentiated cells restricted to the stump (Dinsmore, 1991). The dramatic effects of apoptosis inhibition, i.e., the absence of the blastema-like formation and the inhibition of head regeneration, suggest a role for apoptosis in the initiation of the head regeneration program in wild-type *Hydra*.

Wnt3/β-Catenin Signaling Provides Mitogenic Signals that Synchronize Cell Cycling

The fact that cells labeled with BrdU before or immediately after amputation then synchronously divide between 2 and 4 hpa in region2 suggested that these cells are subject to strong mitogenic signals, propagated from the apoptotic region. Wnt3 produced by the apoptotic cells is well positioned to serve this function. As Wnt3 is well known to be required for head regeneration (Lengfeld et al., 2009), it will be interesting to see if future studies demonstrate that this function is dependent in part upon the proliferative effects described here.

The cycle length is about 24 hr for i-cells in homeostatic conditions; however, this length may be dramatically reduced under conditions of rapid growth with a decreased G2 and an increase in stem cell self-renewal (Holstein and David, 1990). If i-cells that enter S phase upon amputation do in fact divide 4 hr later, this would entail a very short S phase (down to 3 hr) directly followed by mitosis. Alternatively, progenitors already in late S phase at the time of amputation might be preferentially attracted toward the wound and thus ready to rapidly divide. In the lower body column (region3), the BrdU+ cells labeled after amputation also appear to divide synchronously, but 2 hr later than in region2, suggesting that they receive or respond to the synchronization signal with delay. Interestingly, a similar correlation between activation of the canonical Wnt pathway and i-cell proliferation was previously reported by Teo et al. (2006), who studied stem cell fate determination in *Hydractinia*, a cnidarian species closely related to *Hydra*.

A Dual Role for Wnt3 Signaling during Early Head Regeneration?

Previous work showed the upregulation of *Wnt3* expression several hours after mid-gastric section in endodermal epithelial cells (Hobmayer et al., 2000; Guder et al., 2006a), whereas this work identified an immediate and transient overproduction of Wnt3 protein by cells of the interstitial lineage. These two types of regulation actually appear to take place sequentially, as we could confirm the significant increase in *Wnt3* expression

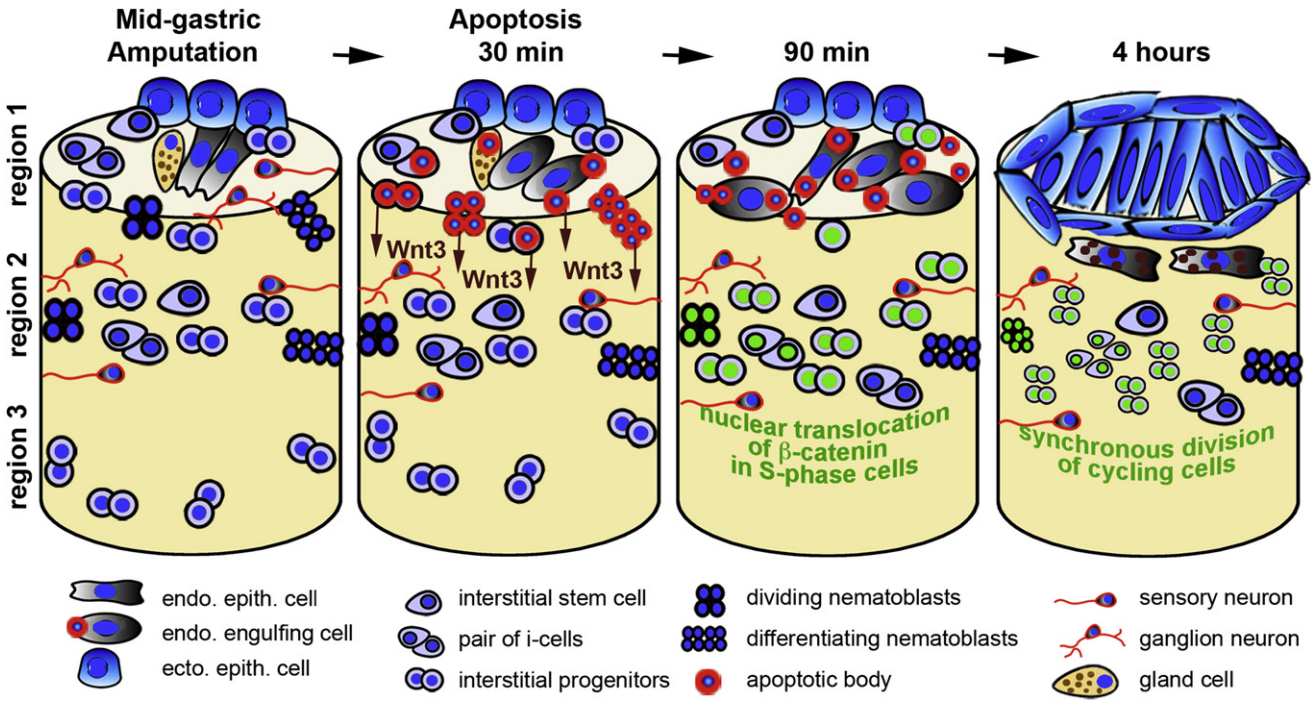

Figure 7. Schematic View of the Early Cellular Remodeling Induced by Mid-Gastric Section in *Hydra* Head-Regenerating Halves

The apoptotic cells from region1 transiently release Wnt3; this release leads S phase cells (predominantly pairs of i-cells and interstitial progenitors) in region2 to activate β-catenin and undergo synchronous division at 4 hr. S phase cells may also be recruited to the wound site via migration from distal sites (see Discussion). By 4 hpa, the apoptotic cells have been engulfed and removed by endodermal epithelial cells, which themselves now express Wnt3 (brown dots). The ectodermal epithelial cells have stretched to cover the wound.

between 2 and 3 hpa and we detected high levels of Wnt3 protein in endodermal epithelial cells at 4 hpa, as previously reported. Therefore, we think that the Wnt3 pathway is activated by two distinct regulatory mechanisms after mid-gastric section, an immediate and transient one, detected at the protein level in the apoptotic cells of the tip, and a later one, i.e., after 2 hpa, involving gene regulation in the endodermal epithelial cells. The dramatic Wnt3 increase detected between 15 min and 1 hpa is assumed to rely mostly on translational and/or posttranslational regulation that would promote the rapid production of Wnt3 by the apoptotic cells. Complex regulation of Wnt3 secretion that relies on Wnt3 acylation is currently emerging (Bartscherer and Boutros, 2008); it might also be at work in *Hydra* regenerating their heads.

Morphallactic versus Epimorphic Regeneration in *Hydra*

Hydra do regenerate when mitosis is inhibited (Park et al., 1970), and BrdU analyses performed on "nerve-free" *Hydra* showed the absence of S phase cells in HR tips over the first 12 hpa (Holstein et al., 1991). Indeed, even in wild-type *Hydra* we think that regeneration can follow several routes, as head regeneration after decapitation does not require apoptosis (S.C., unpublished data). The data presented here therefore show that more than one mechanism contributes to head regeneration in *Hydra*, and that some of the relevant pathways display striking similarities with epimorphic regeneration in bilaterians, which relies on blastema formation, either through migration of proliferating stem cells toward the wound as in planarians, or dedifferentiation of differentiated cells and recruitment of local stem cells as in vertebrates (Sánchez Alvarado and Tsonis, 2006). Thus, it appears that according to the cellular context animals deploy different modes of regeneration to activate shared effectors (such as Wnt3).

Apoptosis as a Driving Force for Regeneration

Caspase-dependent cell death (apoptosis) has been reported in several developmental contexts where cellular remodelling is required: during regeneration in newt (Vlaskalin et al., 2004), *Xenopus* (Tseng et al., 2007), and planarians (Hwang et al., 2004), but also during metamorphosis in *Hydractinia* larvae (Seipp et al., 2001), ascidians, and amphibian tadpoles (Nakajima et al., 2005). Whether the apoptotic cells convey some signaling in these contexts remains unknown. In contrast, in *Drosophila* imaginal discs, apoptotic cells produce Wnts and BMPs to promote compensatory proliferation of surrounding cells (Huh et al., 2004; Perez-Garijo et al., 2004; Ryoo et al., 2004), very similarly to the *Hydra* process reported here. However, these studies did not show the apoptosis-dependent synchronization of S phase cells. Studies in which FR tips are converted to HR tips suggest that the presence of a large number of apoptotic cells coordinately regulates Wnt3 signaling, the recruitment of cycling cells, their synchronization to divide, and the triggering of a complete regeneration process. This mechanism might be relevant for other regenerative processes where the amplitude of the initial apoptosis is critical for launching the regenerative program (Nir et al., 2007). More recent work showed that dying

cells in the *Drosophila* eye disc actually activate distinct signaling pathways according to their differentiation status: progenitor cells activate the Wnt pathway, whereas differentiated cells such as neurons activate the Hedgehog pathway (Fan and Bergmann, 2008). Interestingly the former cells make use of the initiator caspase Dronc, whereas the latter make use of effector caspases, suggesting distinct nonapoptotic functions for each class of caspase. In *Hydra*, it remains to be determined whether Wnt3 production is under the control of initiator and/or effector caspases.

EXPERIMENTAL PROCEDURES

Hydra Culture

Hydra vulgaris (*Hv*, Basel strain) and the transgenic Icy1 AEP *Hydra* (gift from Thomas Bosch) were cultured in *Hydra* medium (HM) as in Chera et al. (2006). Unless stated, all regeneration experiments were performed at 18°C on polyps gently detached from their parents, starved for 3 days, bisected at mid-gastric level, and kept in 1 ml HM/*Hydra*.

Maceration

Ten intact body columns or regions from 20 regenerating halves sliced as in Figure 1A were macerated (Chera et al., 2007). For Icy-1 *Hydra*, tissues were macerated for 15 min in 50 μl of 7% glycerol, 7% acetic acid, fixed in 4% PFA for 15 min, spread on electrically charged slides, and dried ON in the dark.

Detection of Apoptosis

In Situ Cell Death Detection Kit Fluorescein (Roche) was used for TUNEL assays. The dried macerated slides were washed 3 × 10 min in PBS, treated for 2 min in 0.2% sodium citrate, 0.5% Triton X-100 fresh solution at RT, heated for 30 min at 70°C, and washed 5 min in PBS. After adding 50 μl TUNEL reaction mixture, the slides were incubated in a humid dark chamber for 1 hr at 37°C, washed 3 × 10 min in PBS, counterstained 10 min with Hoechst 33342 (1 μg/ml) and MitoFluor598 (Molecular Probes, 200 nM), and mounted in Mowiol. Whole-mount *Hydra* were fixed ON in 4% PFA, washed 3 × 10 min in PBS, treated for 10 min in 0.5% sodium citrate/0.5% Triton X-100 at RT, heated for 10 min at 70°C, washed 5 min in PBS, incubated in the TUNEL mixture at 37°C for 90 min, washed 2 × 10 min in PBS, stained in Hoechst, and mounted in Mowiol. Annexin-V-Cy5 Apoptosis Detection Kit (BioVision) was used on ten regenerating tips incubated for 15 min in 50 μl 7% glycerol, 7% acetic acid, 85% Annexin-V binding buffer, and 1% Annexin-V-Cy5. The cell suspension was then fixed in 4% PFA for 15 min, spread on gelatin slides, dried, and immunodetected.

Immunochemistry

Whole-mount *Hydra* were briefly relaxed in 2% urethane and fixed ON in Lavdowsky1 (50% ethanol, 3.7% formaldehyde), washed 3 × 10 min in PBS, treated for 1 hr with 3% H_2O_2, blocked in 2% BSA, incubated ON at 4°C in the anti-Wnt3 antibody (SantaCruz sc-5212, 1/50), washed 3 × 10 min in PBS, exposed to anti-goat-HRP (Promega, 1/100) for 4 hr, and detected with tyramide (Invitrogen) as in Miljkovic-Licina et al. (2007). For the secondary detection, peroxidase activity was blocked ON in 3% H_2O_2, and anti-β-catenin (Abcam ab19450, 1/100) was added ON at 4°C and tyramide detected. For phosphoHistone H3, *Hydra* were fixed in Helly fixative for 24 hr at 4°C, washed in water, dehydrated ON at 4°C in methanol, progressively rehydrated with PBS, denatured in HCl 2N for 30 min at RT, washed in PBS, and immunodetected with anti-PhosphoHistone H3 (Upstate Inc, 1/100). Immunodetection on macerates used anti-CREB (clone 81524, 1/4000) and anti-RSK (BD Transduction Laboratories, R23820, 1/1000) as in Chera et al. (2007) or anti-Wnt3 as above.

BrdU Detection

Hydra were BrdU-labeled in 5 mM BrdU/HM (Sigma) for 15 min (BrdU/β-catenin colocalization) or 2 hr (BrdU/CREB codetection), then either fixed in PFA4% or macerated. Whole-mounts were treated 20 min in 2N HCl at RT, washed in PBS 3 × 5 min, and blocked 2 hr in BSA 2%. The anti-BrdU (Roche Kit III, 1/20) and anti-β-catenin (1/100) antibodies were sequentially HRP-tyramide-detected. For BrdU and CREB detection, *Hydra* were incubated ON at 4°C in the mixed anti-BrdU (1/20), anti-hyCREB (1/4000) antibodies. Samples were PBS washed, incubated 4 hr at RT in the mixed anti-mouse AlexaFluor488 and anti-rabbit AlexaFluor555 (Molecular Probes, 1/600), PBS washed, DAPI-stained, and mounted in Mowiol. The samples were analyzed on Leica TCS SP2 confocal, and nuclear counting was performed on squared snapshots (l: 170 μm). Macerates, spread on electrically charged slides, were BrdU-detected as above.

Western Blot

The anti-Wnt3 and anti-β-catenin antibodies were biotinylated (Kaloulis et al., 2004) and used 1/200 on the in vitro produced *Hydra* Wnt3 protein (Promega) or on WCE from 50 *Hydra* exposed 3× to dsRNAs, and detected with biotin-HRP (WB 1:5000). Tubulin, as loading control, was detected with the anti-tubulin antibody (Sigma T5168, 1/4000) and anti-mouse-HRP (Promega, 1/10,000).

Drug Treatments and Regeneration Experiments

Hydra were exposed to drugs from 90 min before bisection up to 1 or 2 hpa. ZVAD(OMe)-FMK (Alexis) was given to 3 × 15 *Hydra* in 0.5 ml HM/*Hydra* and washed out at 1 hpa, and regeneration was continued over 72 hr to record emergence of tentacle buds or peroxidase activity at the basal disk (Hoffmeister and Schaller, 1985). ZVAD-treated animals were also macerated at 2 hpa to control the level of apoptosis or exposed to BrdU after bisection and fixed at 1 and 4 hpa. For the Wnt3 rescue experiment, 50 *Hydra* per condition were exposed to ZVAD plus Wnt3 protein (R&D Systems) in glassware, amputated, and kept in 1 ml up to 2 hpa, then washed in HM, and either fixed for immunodetection or transferred to dishes to continue regeneration as usual.

Ectopic Apoptosis and the Splitting Assay

After bisection the upper halves were kept in HM for 15 min and transferred in an agar-coated dish with preformed 0.5 × 0.3 × 0.3 mm cavities in a minimal amount of HM. A glass capillary flame-heated until it becomes red was used to briefly touch the FR tip 1–3 times under binocular. The amount of heat required for inducing apoptosis provoked a brief contraction but no tissue dissociation. Those halves (3 × 20) were then either ZVAD-treated and left to regenerate, or fixed at 1 hpa, or immediately exposed to BrdU and fixed at 1 or 4 hpa. For the splitting assay, FR halves were heat-treated as above, left to regenerate for either 30 min or 2 hr when exposed to BrdU, and longitudinally split with a scalpel in two symmetrical halves. For each animal, one half was allowed to heal and regenerate while the other half was fixed and immunodetected.

Cloning and Semiquantitative RT-PCR

The *Wnt3* and *β-catenin Hv* cDNAs were isolated by RT-PCR, 687 and 720 bp long, respectively (Table S1), with the QuickPrep micro-mRNA Purification (GE Healthcare) and Sensiscript (QIAGEN) kits. For semiquantitative RT-PCR, RNA was prepared from five intact *Hydra* or ten regenerating halves after removing either basal disk or head, 50 ng was reverse transcribed as above, and amplified over 20 and 24 cycles, 14 cycles for the actin control.

RNAi Experiments

The *Hv_Wnt3-687* and *Hv_β-catenin-720* cDNAs were inserted into the L4440 double T7 vector. This empty vector, which upon IPTG induction produces a 183 bp dsRNA, was used as negative control in every experiment. *Hydra* were exposed to dsRNAs every other day as in Chera et al. (2006) with minor modifications (Buzgariu et al., 2008). The silencing efficiency was controlled by RT-PCR analysis on ten regenerating halves per condition.

SUPPLEMENTAL DATA

Supplemental Data include eight figures and nine tables and can be found with this article online at http://www.cell.com/developmental-cell/supplemental/S1534-5807(09)00298-6.

ACKNOWLEDGMENTS

We thank T. Bosch and K. Khalturin for the generous gift of the transgenic Icy1 strain, Y. Shimazaki for help with TEM, I. Rodriguez, M. Crescenzi, M. Torres, P. Bossert, and Z. Zachar for helpful discussions and/or critical reading, and an

anonymous reviewer for precious advice. The laboratory is funded by the Swiss National Foundation, the Geneva State, the NCCR "Frontiers in Genetics" Stem Cells & Regeneration pilot project, the Claraz Donation, and the Academic Society of Geneva.

Received: August 6, 2008
Revised: April 6, 2009
Accepted: July 20, 2009
Published: August 17, 2009

REFERENCES

Bartscherer, K., and Boutros, M. (2008). Regulation of Wnt protein secretion and its role in gradient formation. EMBO Rep. *9*, 977–982.

Bottger, A., and Alexandrova, O. (2007). Programmed cell death in Hydra. Semin. Cancer Biol. *17*, 134–146.

Broun, M., Gee, L., Reinhardt, B., and Bode, H.R. (2005). Formation of the head organizer in hydra involves the canonical Wnt pathway. Development *132*, 2907–2916.

Buzgariu, W., Chera, S., and Galliot, B. (2008). Methods to investigate autophagy during starvation and regeneration in hydra. Methods Enzymol. *451*, 409–437.

Chera, S., de Rosa, R., Miljkovic-Licina, M., Dobretz, K., Ghila, L., Kaloulis, K., and Galliot, B. (2006). Silencing of the hydra serine protease inhibitor Kazal1 gene mimics the human Spink1 pancreatic phenotype. J. Cell Sci. *119*, 846–857.

Chera, S., Kaloulis, K., and Galliot, B. (2007). The cAMP response element binding protein (CREB) as an integrative HUB selector in metazoans: clues from the hydra model system. Biosystems *87*, 191–203.

Cikala, M., Wilm, B., Hobmayer, E., Bottger, A., and David, C.N. (1999). Identification of caspases and apoptosis in the simple metazoan Hydra. Curr. Biol. *9*, 959–962.

David, C.N. (1973). A quantitative method for maceration of hydra tissue. Wilhelm Roux Archiv. *171*, 259–268.

Dinsmore, C.E. (1991). A History of Regeneration Research (Cambridge, UK: Cambridge University Press).

Fan, Y., and Bergmann, A. (2008). Distinct mechanisms of apoptosis-induced compensatory proliferation in proliferating and differentiating tissues in the Drosophila eye. Dev. Cell *14*, 399–410.

Fujisawa, T. (2003). Hydra regeneration and epitheliopeptides. Dev. Dyn. *226*, 182–189.

Fujisawa, T., and David, C.N. (1984). Loss of differentiating nematocytes induced by regeneration and wound healing in Hydra. J. Cell Sci. *68*, 243–255.

Fujisawa, T., David, C.N., and Bosch, T.C. (1990). Transplantation stimulates interstitial cell migration in hydra. Dev. Biol. *138*, 509–512.

Galliot, B., Welschof, M., Schuckert, O., Hoffmeister, S., and Schaller, H.C. (1995). The cAMP response element binding protein is involved in hydra regeneration. Development *121*, 1205–1216.

Galliot, B., Miljkovic-Licina, M., de Rosa, R., and Chera, S. (2006). Hydra, a niche for cell and developmental plasticity. Semin. Cell Dev. Biol. *17*, 492–502.

Guder, C., Philipp, I., Lengfeld, T., Watanabe, H., Hobmayer, B., and Holstein, T.W. (2006a). The Wnt code: cnidarians signal the way. Oncogene *25*, 7450–7460.

Guder, C., Pinho, S., Nacak, T.G., Schmidt, H.A., Hobmayer, B., Niehrs, C., and Holstein, T.W. (2006b). An ancient Wnt-Dickkopf antagonism in Hydra. Development *133*, 901–911.

Hobmayer, B., Rentzsch, F., Kuhn, K., Happel, C.M., von Laue, C.C., Snyder, P., Rothbacher, U., and Holstein, T.W. (2000). WNT signalling molecules act in axis formation in the diploblastic metazoan Hydra. Nature *407*, 186–189.

Hoffmeister, S.A.H., and Schaller, H.C. (1985). A new biochemical marker for foot-specific cell differentiation in hydra. Roux Arch. Dev. Biol. *194*, 453–461.

Holstein, T.W., and David, C.N. (1990). Cell cycle length, cell size, and proliferation rate in hydra stem cells. Dev. Biol. *142*, 392–400.

Holstein, T.W., Hobmayer, E., and David, C.N. (1991). Pattern of epithelial cell cycling in hydra. Dev. Biol. *148*, 602–611.

Huh, J.R., Guo, M., and Hay, B.A. (2004). Compensatory proliferation induced by cell death in the Drosophila wing disc requires activity of the apical cell death caspase Dronc in a nonapoptotic role. Curr. Biol. *14*, 1262–1266.

Hwang, J.S., Kobayashi, C., Agata, K., Ikeo, K., and Gojobori, T. (2004). Detection of apoptosis during planarian regeneration by the expression of apoptosis-related genes and TUNEL assay. Gene *333*, 15–25.

Kaloulis, K., Chera, S., Hassel, M., Gauchat, D., and Galliot, B. (2004). Reactivation of developmental programs: the cAMP-response element-binding protein pathway is involved in hydra head regeneration. Proc. Natl. Acad. Sci. USA *101*, 2363–2368.

Khalturin, K., Anton-Erxleben, F., Milde, S., Plotz, C., Wittlieb, J., Hemmrich, G., and Bosch, T.C. (2007). Transgenic stem cells in Hydra reveal an early evolutionary origin for key elements controlling self-renewal and differentiation. Dev. Biol. *309*, 32–44.

Lengfeld, T., Watanabe, H., Simakov, O., Lindgens, D., Gee, L., Law, L., Schmidt, H.A., Ozbek, S., Bode, H., and Holstein, T.W. (2009). Multiple Wnts are involved in Hydra organizer formation and regeneration. Dev. Biol. *330*, 186–199.

MacWilliams, H.K. (1983). Hydra transplantation phenomena and the mechanism of Hydra head regeneration. II. Properties of the head activation. Dev. Biol. *96*, 239–257.

Miljkovic-Licina, M., Chera, S., Ghila, L., and Galliot, B. (2007). Head regeneration in wild-type hydra requires de novo neurogenesis. Development *134*, 1191–1201.

Murate, M., Kishimoto, Y., Sugiyama, T., Fujisawa, T., Takahashi-Iwanaga, H., and Iwanaga, T. (1997). Hydra regeneration from recombined ectodermal and endodermal tissue. II. Differential stability in the ectodermal and endodermal epithelial organization. J. Cell Sci. *110*, 1919–1934.

Nakajima, K., Fujimoto, K., and Yaoita, Y. (2005). Programmed cell death during amphibian metamorphosis. Semin. Cell Dev. Biol. *16*, 271–280.

Nir, T., Melton, D.A., and Dor, Y. (2007). Recovery from diabetes in mice by beta cell regeneration. J. Clin. Invest. *117*, 2553–2561.

Park, H.D., Ortmeyer, A.B., and Blankenbaker, D.P. (1970). Cell division during regeneration in Hydra. Nature *227*, 617–619.

Perez-Garijo, A., Martin, F.A., and Morata, G. (2004). Caspase inhibition during apoptosis causes abnormal signalling and developmental aberrations in Drosophila. Development *131*, 5591–5598.

Ryoo, H.D., Gorenc, T., and Steller, H. (2004). Apoptotic cells can induce compensatory cell proliferation through the JNK and the Wingless signaling pathways. Dev. Cell *7*, 491–501.

Sánchez Alvarado, A., and Tsonis, P.A. (2006). Bridging the regeneration gap: genetic insights from diverse animal models. Nat. Rev. Genet. *7*, 873–884.

Seipp, S., Schmich, J., and Leitz, T. (2001). Apoptosis—a death-inducing mechanism tightly linked with morphogenesis in Hydractina echinata (Cnidaria, Hydrozoa). Development *128*, 4891–4898.

Steele, R.E. (2002). Developmental signaling in Hydra: what does it take to build a "simple" animal? Dev. Biol. *248*, 199–219.

Teo, R., Mohrlen, F., Plickert, G., Muller, W.A., and Frank, U. (2006). An evolutionary conserved role of Wnt signaling in stem cell fate decision. Dev. Biol. *289*, 91–99.

Tseng, A.S., Adams, D.S., Qiu, D., Koustubhan, P., and Levin, M. (2007). Apoptosis is required during early stages of tail regeneration in Xenopus laevis. Dev. Biol. *301*, 62–69.

Vlaskalin, T., Wong, C.J., and Tsilfidis, C. (2004). Growth and apoptosis during larval forelimb development and adult forelimb regeneration in the newt (Notophthalmus viridescens). Dev. Genes Evol. *214*, 423–431.